DOE/JPL
Distribution Category UC-63
DOE/JPL-954852-79/1

(NASA-CR-158572) STRUCTURE AND ELECTRICAL ACTIVITY OF PLANAR DEFECTS IN EFG RIBBONS Quarterly Report, 1 Jan. - 31 Mar. 1979 (Cornell Univ., Ithaca, N. Y.) 11 p HC A02/MF A01 CSCL 20L G3/76

N79-23806

Unclas
25188

Department of Material Science
Cornell University
Bard Hall
Ithaca, N.Y. 14853

Structure and Electrical Activity of Planar Defects in EFG Ribbons

Prepared by
D.G. Ast

First Quarterly Report - JPL Contract No. 954852

Covering Period: January 1st, 1979 - March 31, 1979

April 15, 1979

"The JPL Low-Cost Silicon Solar Array Project is sponsored by the Department of Energy and forms part of the Solar Photovoltqic Conversion Program to initiate a major effort towards the developement of low-cost solar arrays. This work was performed for the Jet Propulsion Laboratory, California Institute of Technology by agreement between NASA and DOE."

ABSTRACT

The structure and electrical activity of planar defects in EFG Silicon was investigated by optical, electron beam induced current (EBIC), and transmission electron microscopy (TEM).

What appears to be twin boundaries by both optical microscopy + etching, and by EBIC are in reality systems of microtwins, some of which are only a few atomic lattice planes thick.

The electrical activity of planar defects appears to be correlated with emission of dislocations especially at termination points. Impurity effects may also play a rôle. Twin boundaries per se appear not to be electrically active.

TABLE OF CONTENTS

1) Material and Methods

The material was EFG ribbons produced by IBM. As received material had a slightly hazy appearance, probably caused by a surface layer of SiC generated by the silicon-die interaction (not investigated). The specimens were polished with Syton to remove the surface layer and to obtain optically flat surfaces. After polishing, specimens were examined by optical microscopy. Regions which contained interesting linear defect structures were then selected for investigation of their electrical activity via electron beam induced current microscopy (EBIC). Approximately 1x1 cm specimen were cut out on which 4 square Schottky Diodes of approximately 4x4mm were prepared by the RF sputter deposition of 300 Å of Ti. After EBIC, the Ti was removed by etching and areas with interesting electrical activity were selected for subsequent transmission electron microscopy (TEM) by chemical thinning. The remainder of the specimen was Sirtl etched in order to correlate the EBIC activity with structural features as revealed by etching.

2) Results

The overwhelming majority of the planar defects were coherent twin boundaries parallel to the approximately [122] growth direction of the ribbon and perpendicular to its (110) surface (see figure 1). High angle grain boundaries were rarely found. Besides numerous single dislocations, fairly regular dislocation arrays (i.e. small angle grain boundaries) were occasionally observed.

The most interesting results obtained were those from coherent twin boundaries. EBIC studies showed that EBIC contrast along these boundaries was frequently discontinuous, indicating that coherent twin boundaries per se are not electrically active. High resolution multibeam TEM (Fig. 2) showed that what appeared to be twin boundaries by etching or EBIC consisted in reality a system of microtwins. These microtwins, some of which are only a few atomic lattic planes thick form the majority of the planar defects observed in the sample. Fig. 2 shows 2 such microtwins. The view in Fig. 2 is along the open [110] channels, as shown in the insert, the borders of which are approximately parallel to the two [111] directions in the plane of the figure. Growth direction of the ribbon is parallel to the long dimension of the twins. In addition to the three coherent twins (lower half), Figure 2 shows also an example of an incoherent twin boundary on a (211) plane which extends from the upper (visible) to the lower surface (not visible in Fig. 2) of the specimen. The contrast of this boundary indicates a translational shift of about 1 Å between the two adjoining crystals. A burgers circuit around the incoherent twin boundary (taken from a full picture) shows that this boundary also contains a dislocation. Generally, the closure failure of such circuits is $\Sigma\, b_i \approx 0$, which indicates that these twin defects are in a low energy configuration. Microtwins ending in the crystal act as dislocation sources (Fig. 3). Such microtwins tend to be electrically active. Microtwins can also terminate in planar faults, (as can be seen in Fig. 4) which shows one microtwin precisely edge on (arrow). Such defects tend also to be elctrically active. In principe, the electrical activity of twin boundaries can be either caused by impurity segregation to the boundpoint's (Fig. 3). Results to date favor the latter explanation. No impurity precipitates were dedected but impurity effects can not be ruled out with certainity since small concentration of impurities are exceedingly difficult to detect.

Appendices

1) Program Plan

Previous Program Plan is in effect.

2) <u>Man Hours and Costs</u>

Cumulative manhours to date are 200 hours, with manhours for the first quarter at 50. Costs to date are $976.

3) <u>Engineering drawings and sketches Generated during the Reporting Period</u>.

None

4) <u>Summary of Characterization data Generated during Reporting Period</u>.

See abstract, this report.

5) <u>Action Items required by JPL</u>

None

6) <u>New Technology</u>

None

FIGURE CAPTIONS

Figure 1. Optical Micrograph of polished IBM prepared EFG ribbon. Magnification x100. Growth direction is vertical.

Figure 2. High resolution TEM micrograph of microtwins in EFG ribbons. Lower half shows three coherent twins edge on. Note that some twins are only a few atomic (111) planes thick. Upper half shows incoherent twin running on a (211) from upper surface (left, visible) to lower surface (not visible on this micrograph). A burgers vector circuit around the full defect shows that this fault also contains a dislocation.

Figure 3. Dislocation network associated with terminating microtwin.

Figure 4. Microtwin (Arrow A) viewed edge on, terminating in planar defects.

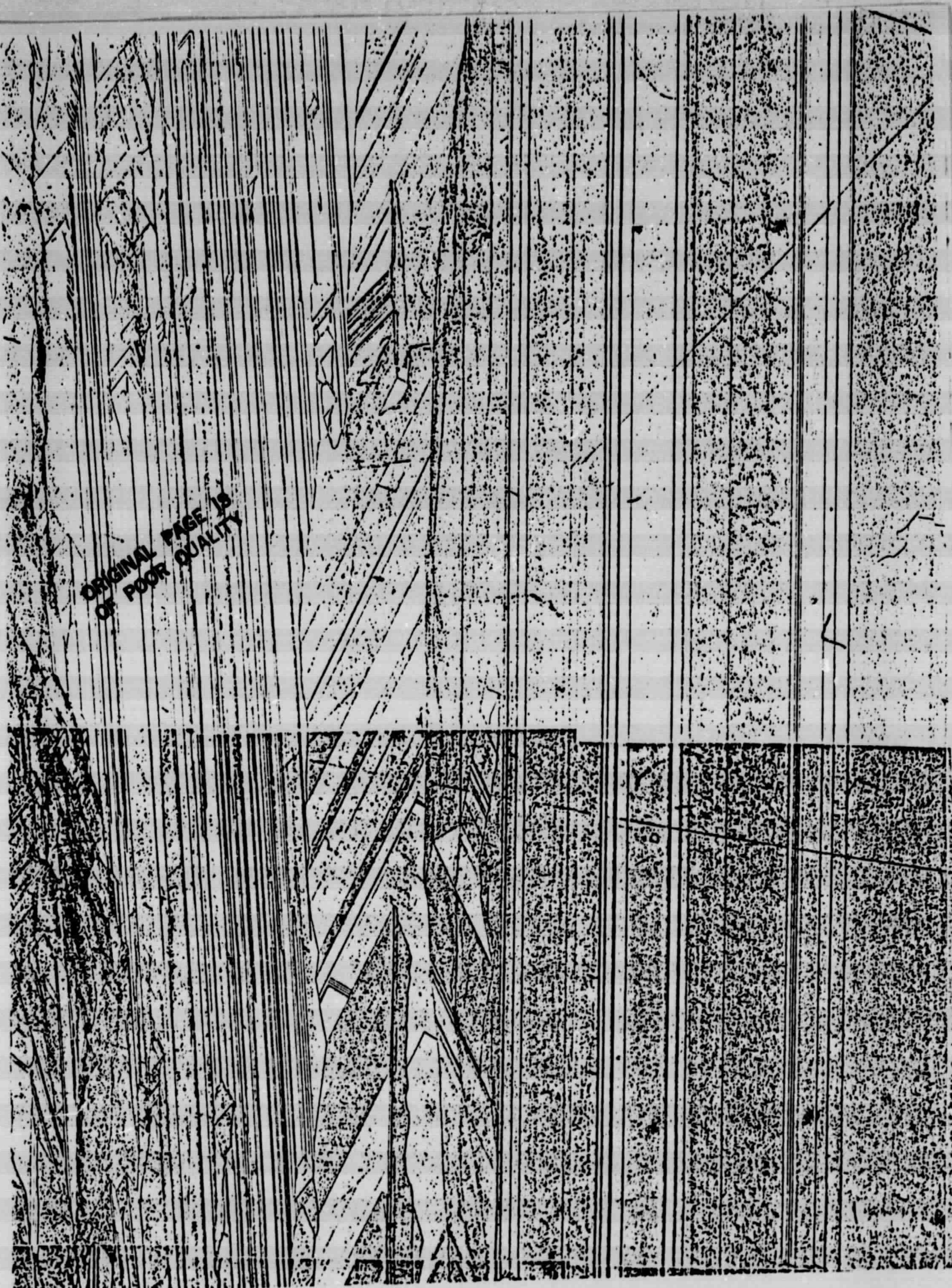

x 100

Fig. 1

x 3 200 000

Fig. 2

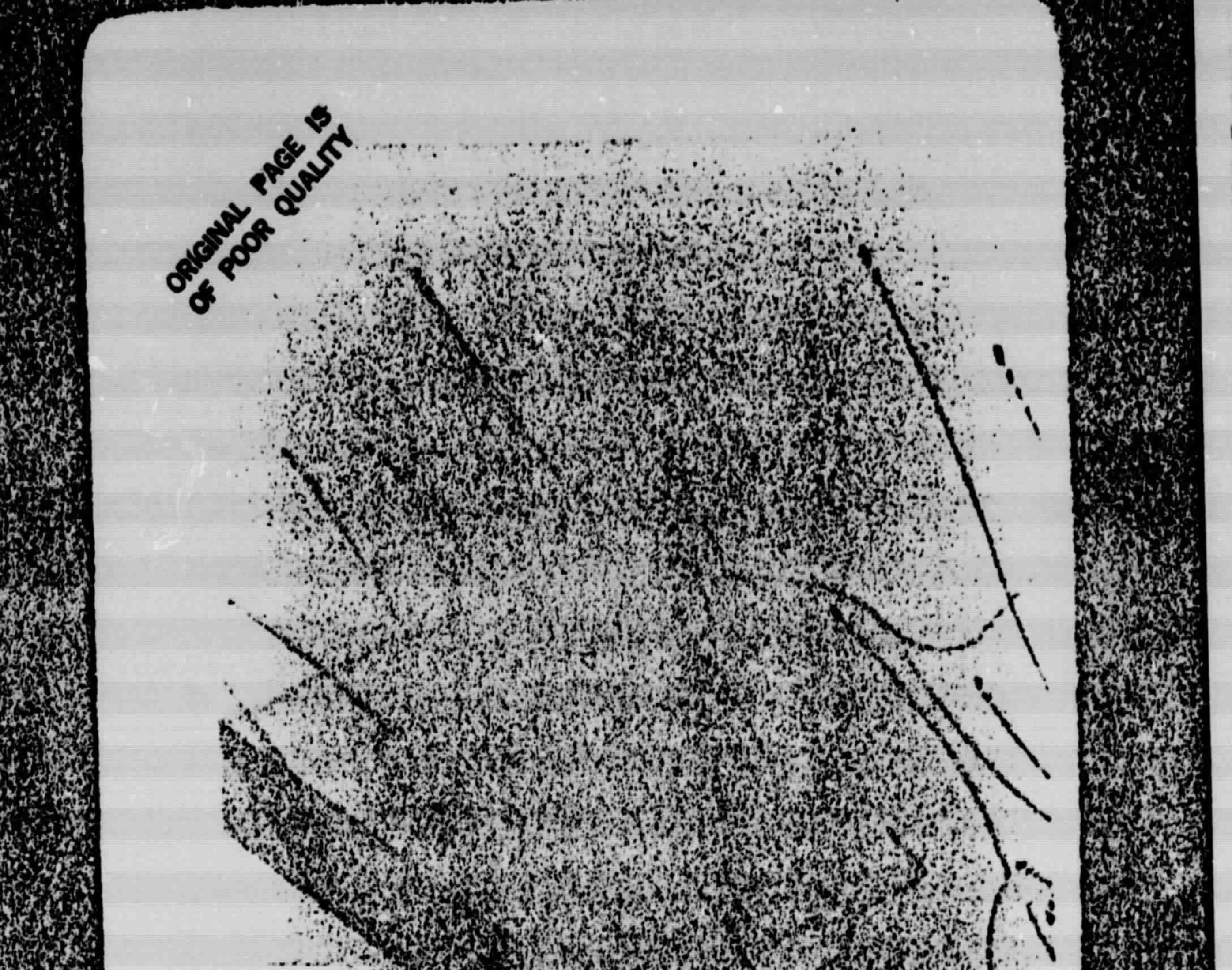

x 25 000

Fig 3

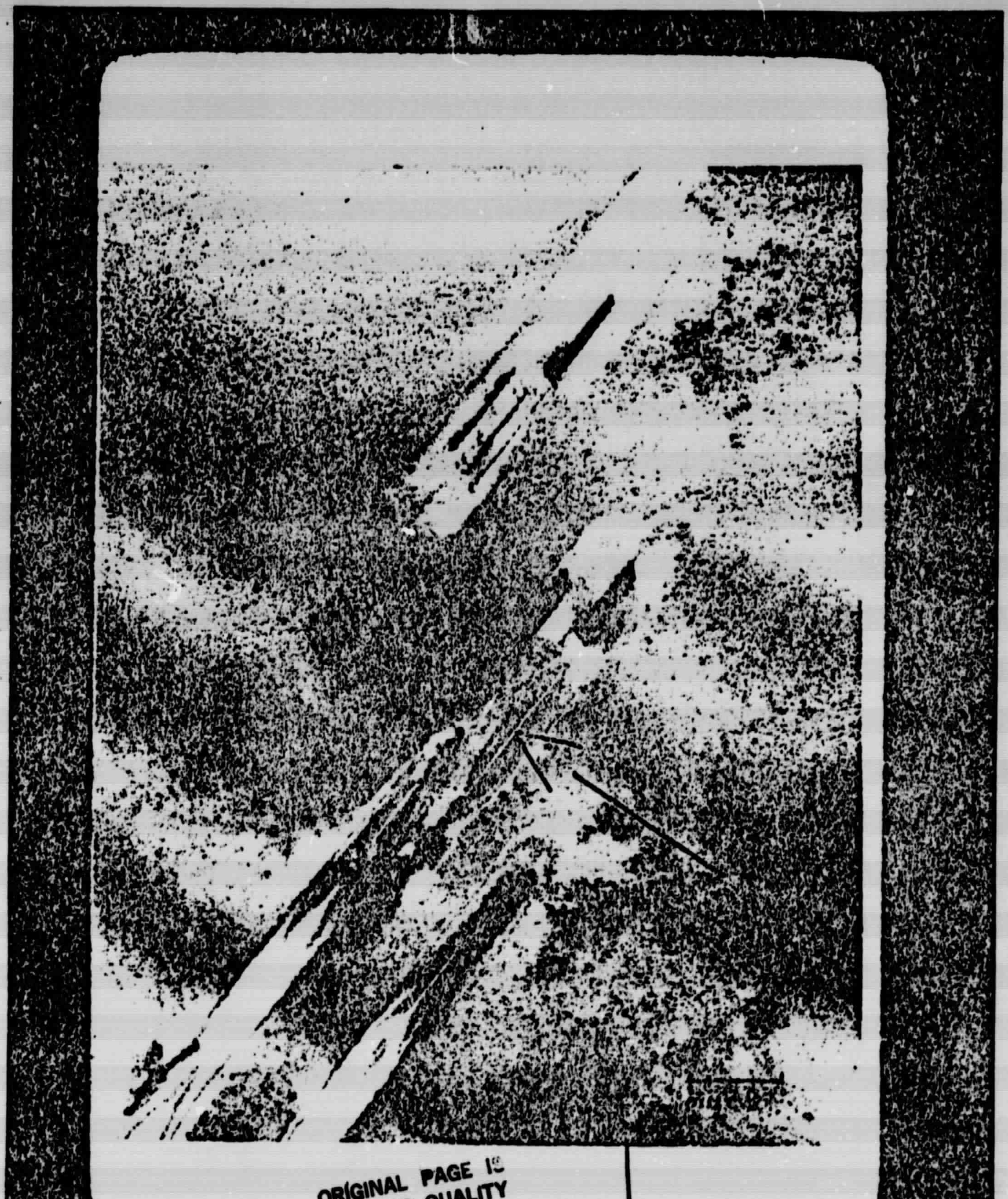

x 35 000

Fig 4